

Conventional 2D-EPI or Segmented 3D-EPI? A Temporal SNR Study at 3 and 7 Tesla

Rüdiger Stirnberg¹ and Tony Stöcker¹

¹German Center for Neurodegenerative Diseases (DZNE), Bonn, Germany

Target Audience: This work is primarily targeted at neuroscientists and MR physicists focusing on high resolution functional MRI applications.

Purpose: Recently, segmented 3D-EPI has been proposed for application of BOLD functional MRI at ultra-high fields such as 7 Tesla¹. Unfortunately, the statistical power, especially of 3D-EPI time series data, is limited by physiological noise (signal fluctuations due to breathing, etc.): with increasing base SNR the temporal SNR ($tSNR = \text{AVG}/\text{STD}$ with respect to time) tends towards a constant value, which is smaller the more shots per EPI-volume are required². This work compares the $tSNR$ and signal sensitivity ($tSNR/\text{Vacquisition time}$) characteristics of 2D-EPI vs. 3D-EPI under “real-life” conditions, i.e. for different low- and high resolution protocols for fast fMRI data acquisition at 7 and 3 Tesla.

Methods: All experiments were performed on Siemens (Erlangen) MRI scanners, 3T Skyra and Magnetom 7T, both utilizing a 32 channel head array for signal reception. At 7T RF transmission was performed using a birdcage coil surrounding the receive array. For each field strength (3T/7T) four “low-” (3mm/2mm isotropic) and four “high-resolution” (1.5mm/1mm isotropic) whole brain protocols were prepared according to Table 1 based on a conventional slice-selective 2D-EPI sequence (a) and a custom 3D-EPI sequence with three different configurations: no slice acceleration (b), acceleration by means of parallel imaging (PI) and/or partial Fourier acquisition (c) and optimized for high sensitivity (d). The latter utilized a simple water excitation method based on a single rectangular pulse proposed recently³ in order to reduce “dead time” largely caused by fat saturation as in (a-c). With the slice orientation changed to sagittal the primary phase encoding direction was still along anterior-posterior. However, compared to (b,c) the protocol requires more steps in the secondary phase encoding dimension to cover the field-of-view in left-right direction. Temporal SNR computation was performed from 96 images following co-registration and detrending using FSL⁴. The 3mm 2D-EPI protocol (a) at 3T and the corresponding optimized protocol (d) are utilized for bilateral finger tapping fMRI (blocked paradigm: 20s rest/tapping, alternating for 4:20 minutes). GLM statistical analysis was performed using FSL. At no stage smoothing was applied.

Results: Fig. 1 shows representative axial slices on the example of protocols (a) and (d) for the finger tapping fMRI results (left), the $tSNR$ maps at all field strengths and resolutions (center) and example magnitude images for 1mm isotropic resolution at 7T (right). The histograms in Fig. 2 summarize $tSNR$ for all protocol types on the example of 3T.

Discussion: Fig. 1 demonstrates an increase in $tSNR$ at higher spatial resolution for 3D- compared to 2D-EPI, both at 3T and 7T. Furthermore, even though $tSNR$ at 3T and 3mm resolution is reduced, using the optimized 3D-EPI sequence results in a 70% increase of sensitivity due to PI and, therefore, a more robust detection of activation (higher z-scores) and a larger activated volume. The fact that the optimized, PI-accelerated

sagittal protocol results in increased $tSNR$ compared to the corresponding PI-accelerated axial protocol (cf. Fig. 2) is largely due to employing water excitation instead of conventional fat-saturation³ since the latter suffers from signal suppression due to unwanted magnetization transfer effects⁵.

Conclusion: As expected, segmented 3D-EPI has higher $tSNR$ than 2D-EPI at high imaging resolution, which was confirmed at 7T and 3T. However, 3D-EPI is also useful at typical coarse resolutions, as it was shown in the 3T fMRI example. Here, 3D-EPI outperforms conventional slice-selective 2D-EPI, since parallel imaging acceleration in two phase encode directions was applied. This results in a significant sensitivity advantage, which translates to more robust fMRI results. Unexpectedly, the observed $tSNR$ advantage at 7T with 1mm vs. 2mm isotropic resolution was not as clear as at 3T with 1.5mm vs. 3mm, which might be related to different versions of the vendor-provided image reconstruction algorithms at 3T and 7T. The increased sensitivity, however, remains a clear bonus for 3D-EPI at 7T and 3T.

References: [1] Poser et al., NeuroImage 52, 2010; [2] Van der Zwaag et al., Magn. Reson. Med. 67, 2012; [3] Stirnberg et al., Proc. Intl. Soc. ISMRM 21, 2013; [4] Jenkinson et al., NeuroImage 62, 2012, [5] Shin et al., Magn. Reson. Med. 62, 2009

Protocol	3T (TE=30ms)		7T (TE=26ms)	
	3.0mm	1.5mm	2.0mm	1.0mm
(a) 2D-EPI (axial)				
PI factor	-	3	2	3
PF factor	-	-	-	6/8
TR [ms]	2720	6060	3200	8800
(b) 3D-EPI, no slice acc. (axial)				
PI factor	-	3x1	2x1	3x1
PF factor	-	-	-	6/8
TR [ms]	2650	5920	3200	8800
(c) 3D-EPI, slice acc. (axial)				
PI factor	1x2	3x2	2x2	3x2
PF factor	-	-	1x7/8	6/8x7/8
TR [ms]	1330	2920	1400	3800
(d) 3D-EPI, optimized (sagittal)				
PI factor	2x2	2x2	2x2	3x2
PF factor	1x7/8	7/8x6/8	1x6/8	6/8x6/8
TR [ms]	939	2510	1280	3800

Tab. 1 Summary of imaging protocols.

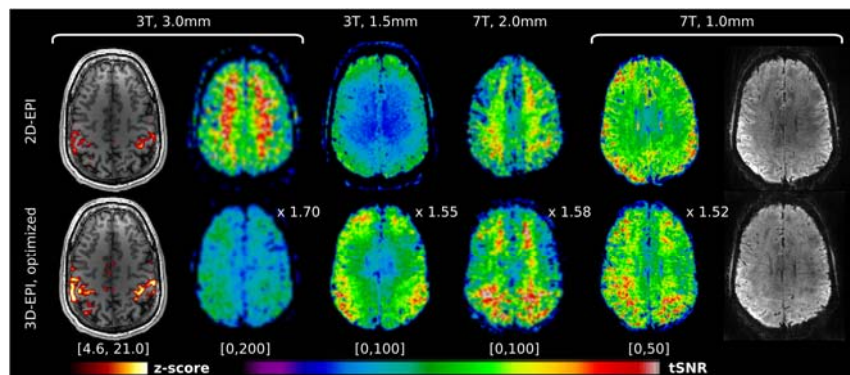


Fig. 1 Left: Detected activation for finger tapping fMRI with conventional 2D-EPI (top) and optimized 3D-EPI (bottom). Center: $tSNR$ maps (numbers in brackets denote the respective ranges). The bottom map values have to be scaled by the indicated factors to account for the increased temporal resolution. Right: example magnitude images at 7T and 1mm isotropic resolution.

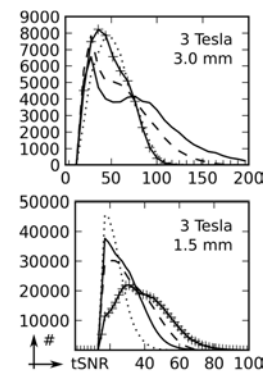


Fig. 2 Histograms of $tSNR$ ignoring different temporal resolutions (solid=a, dashed=b, dotted=c, +=d).